



Learning curve of electromagnetic navigation bronchoscopy for diagnosing peripheral pulmonary nodules in a single institution

Jiayuan Sun^{1,2}, Fangfang Xie^{1,2}, Xiaoxuan Zheng¹, Yifeng Jiang³, Lei Zhu⁴, Xiaowei Mao^{1,2}, Baohui Han²

¹Department of Endoscopy, ²Department of Pulmonary Medicine, ³Department of Radiology, ⁴Department of Pathology, Shanghai Chest Hospital, Shanghai Jiao Tong University, Shanghai 200030, China

Contributions: (I) Conception and design: J Sun, B Han; (II) Administrative support: B Han; (III) Provision of study materials or patients: J Sun, X Zheng; (IV) Collection and assembly of data: F Xie, X Mao; (V) Data analysis and interpretation: J Sun, X Zheng, Y Jiang, L Zhu; (VI) Manuscript writing: All authors; (VII) Final approval of manuscript: All authors.

Correspondence to: Baohui Han. Department of Pulmonary Medicine, Shanghai Chest Hospital, Shanghai Jiao Tong University, 241 West Huaihai Road, Shanghai 200030, China. Email address: xkybhhan@163.com.

Background: Electromagnetic navigation bronchoscopy (ENB) is a novel technology that is designed to diagnose peripheral pulmonary lesions (PPLs). The purpose of the study was to explore the learning curve and evaluate the diagnostic yield and safety of ENB in diagnosing peripheral pulmonary nodules.

Methods: A total of 40 patients discovered with peripheral pulmonary nodules suspicious for malignancy were chronologically enrolled into the study. Biopsy, brushing and flushing specimens were obtained through the extended working channel (EWC). Radial endobronchial ultrasound (R-EBUS) and fluoroscopy were used as means for localization and auxiliary implements in the procedure of ENB. Immunohistochemistry (IHC) and driver genes testing were performed on biopsy samples when it was necessary. All the patients performed chest radiographs to exclude pneumothorax after the procedure. Data of all patients were recorded prospectively and analyzed retrospectively. The learning curve was evaluated using cumulative sum (CUSUM) method.

Results: The mean diameter of the 40 nodules was 21.1±5.3 mm. The average navigation time and total operation time were 8.1±3.2 and 24.6±4.1 min, respectively. The overall diagnostic yield was 82.5% (33/40). CUSUM analysis of learning curve based on the navigation time and total operation time both could be best modeled as polynomials and divided the learning curve into two phases at the point of case 14. The learning curve based on diagnostic yield did not demonstrate an obvious turning point. No complications occurred in the 40 procedures.

Conclusions: ENB is a safe technology with a high diagnostic yield in diagnosing peripheral pulmonary nodules. The learning curve based on the procedure time could be stable after 14 procedures and there was no obvious learning curve based on the diagnostic yield for an experienced pulmonologist.

Keywords: Driver genes testing; electromagnetic navigation bronchoscopy (ENB); immunohistochemistry (IHC); learning curve; peripheral pulmonary nodules

Submitted Jan 16, 2017. Accepted for publication Apr 21, 2017.

doi: 10.21037/tcr.2017.05.39

View this article at: <http://dx.doi.org/10.21037/tcr.2017.05.39>

Introduction

Lung cancer has become the leading cause of cancer death in the world (1). As the popularity of computed tomography (CT) scan for screening lung cancer, the number of pulmonary nodules has been found increasing

substantially. The National Lung Screening Trial Research Team reported 27.3% of high-risk patients who experienced low-dose CT screening had pulmonary nodules suspicious for malignancy (2). Individuals with pulmonary nodules can be evaluated by non-surgical biopsy methods to estimate

the probability of malignancy according to the American College of Chest Physicians (ACCP) Lung Cancer Guidelines, which plays a significant role in the detection of the early lung cancer (3).

The most common non-surgical biopsy methods of diagnosing lung lesions are transbronchial biopsy (TBB) and transthoracic needle aspiration (TTNA) biopsy. However, these two methods are limited either by low accuracy or by potential complications (4-7). Electromagnetic navigation bronchoscopy (ENB) is a promising technology that is designed to guide the biopsy of peripheral pulmonary lesions (PPLs) and increase the diagnostic yield of conventional bronchoscopy. ENB utilizes an electromagnetic technique for real-time navigation based on three-dimensional CT scans and virtual bronchoscopy, which offers an accurate pathway reaching PPLs. ACCP Lung Cancer Guidelines also indicate that in patients with PPLs difficult to reach with conventional bronchoscopy, electromagnetic navigation guidance is recommended if the equipment and the expertise are available (7).

Many previous studies have demonstrated ENB has a high diagnostic yield in diagnosing PPLs (8-10), but few studies explore the learning curve. The study presented our initial experience since its first introduction into the special hospital for thoracic neoplasms, covering a period of about 8 months. The objective of the study was to explore the learning curve and evaluate the diagnostic efficiency and safety of ENB in diagnosing peripheral pulmonary nodules, with the final goal to guide the clinical application of ENB in diagnosing peripheral pulmonary nodules, especially in the newly introduced hospitals.

Methods

Patients

From July 28, 2014 to April 16, 2015 in our Hospital, patients were prospectively enrolled into the clinical study. The inclusion criteria were as follows: (I) all patients were discovered with peripheral pulmonary nodules suspicious of malignancy according to clinical and radiologic features and needed pathologically confirmation; (II) all participants were older than 18 years; (III) chest CT image showed there was bronchus leading to or adjacent to the nodule; (IV) the size of the nodules was no more than 3 cm and beyond the vision of the conventional bronchoscopy. The exclusion criteria were as follows: (I) chest CT image showed pure ground glass opacity (GGO) lesion; (II) severe

cardiopulmonary dysfunction and other indications that cannot tolerate bronchoscopy; (III) refusal of participation. The protocol was approved by the local ethics committee and the ethics approval number was KS1530. All patients participating in the study provided written informed consent and were followed up for at least one year after the procedure.

Procedure

All patients underwent chest CT scans (Philips Brilliance 64 multi-slice spiral CT, Philips Healthcare, The Netherlands) prior to ENB procedures. The data of CT scans met the following criteria for navigation software: (I) slice thickness 1.0 mm; (II) slice interval 0.8 mm; (III) kernel C; (IV) DICOM format; (V) image resolution 512×512. All procedures were performed under local anesthesia and moderate sedation with midazolam and fentanyl and finished by the same operator who was experienced in transbronchial lung biopsy (TBLB) and performed more than 100 cases each year in recent 3 years. ENB (superDimension/inReach system, Covidien, America) procedures were performed as previously described (11,12). A bronchoscope (BF-1T260, Olympus, Tokyo, Japan) with a 2.8 mm diameter biopsy channel was used through the intraoral approach.

When the nodule was reached, the locatable guide (LG) was withdrawn from the extended working channel (EWC) and a radial ultrasound probe (UM-S20-20R, Olympus) was inserted via the EWC to confirm the position of the nodule. Then fluoroscopy was used to confirm the location of the radial ultrasound probe. Specimens were obtained through EWC in the sequence of biopsy and brushing, aided by fluoroscopy to guarantee that the EWC did not dislodge and endobronchial accessories reached the nodule well. After biopsy and brushing, the EWC was flushed with saline to collect liquid specimens. Five biopsy, one brushing and one flushing samples were finally obtained of each nodule. All patients performed chest radiographs after the procedure to exclude pneumothorax. A representative case of ENB guided TBLB was shown in *Figure 1* and an operation video could be available in *Figure 2* (13).

Brushing and flushing specimens were sent for cytological examination and biopsy specimens were processed for histopathological examination. Further immunohistochemistry (IHC), including cytokeratin (CK), thyroid transcription factor-1 (TTF-1), P40 and CD56, was performed if the tumor cannot be classified by morphologic features. Flushing specimens were also processed for

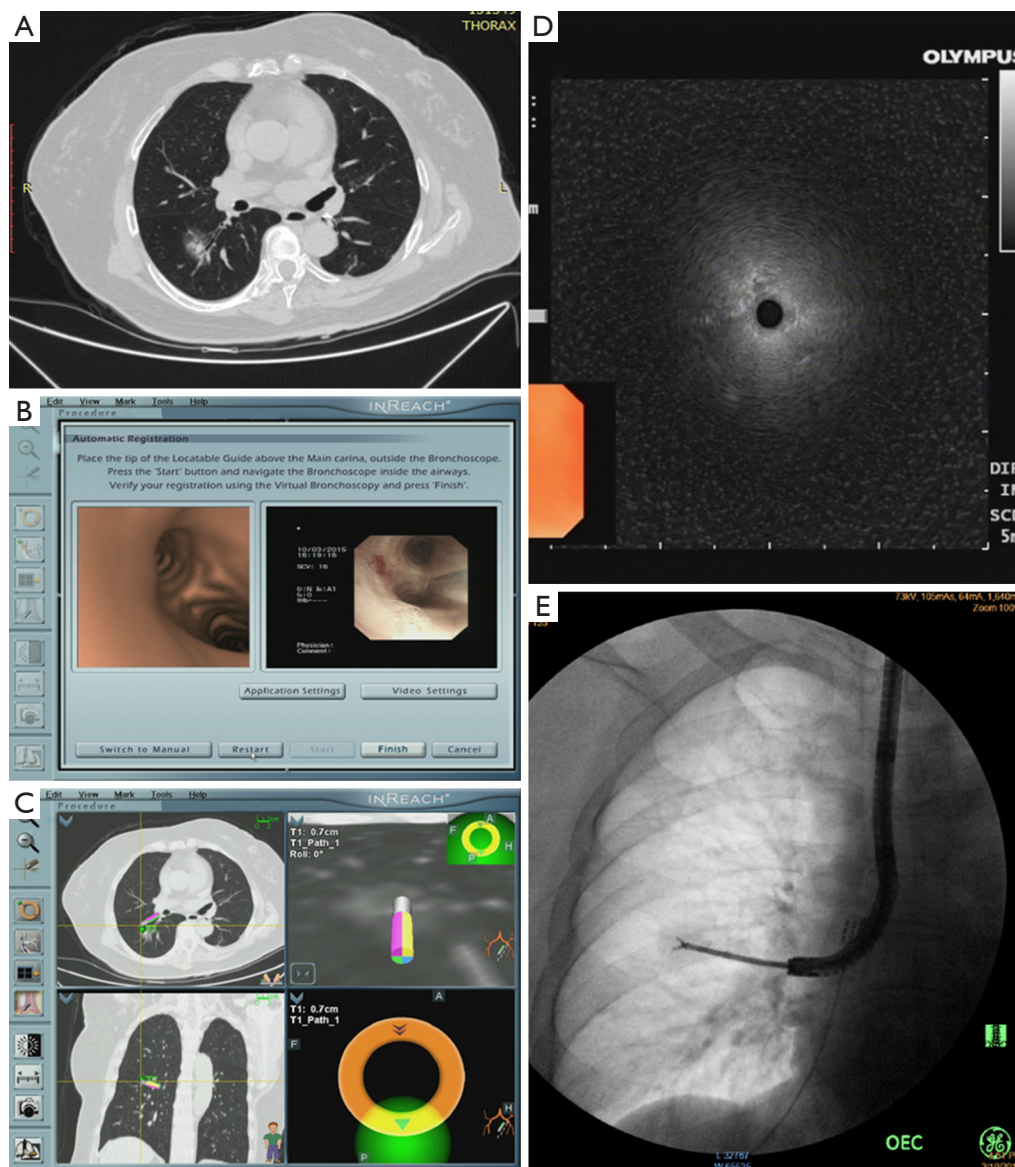


Figure 1 A representative case of ENB guided TBLB. (A) Preoperative CT scan showed a mixed GGO; (B) virtual bronchoscopy image generated after registration was completed; (C) real-time navigation screen when the distance between the sensor probe of the LG and the lesion was nearest; (D) radial ultrasound probe showed mixed blizzard sign; (E) biopsy process under the guidance of fluoroscopy. ENB, electromagnetic navigation bronchoscopy; TBLB, transbronchial lung biopsy; LG, locatable guide; GGO, ground glass opacity; CT, computed tomography.

microbiologic assessment if it was necessary according to the judgment of the doctors. All final diagnoses were made by experienced pathologists. Driver gene testing including epidermal growth factor receptor (EGFR) gene mutations, anaplastic lymphoma receptor tyrosine kinase (ALK) gene fusions and ROS proto-oncogene 1, receptor tyrosine kinase (ROS1) gene fusions performed in nonsquamous

non-small cell lung carcinomas (NSCLCs) which cannot undergo surgery.

Final diagnosis

The final diagnosis of the nodule was based on the histological, cytological pathology or microbiological



Figure 2 Video of ENB-EBUS-X-ray-TBLB procedure (13). The time (00:00:00 to 00:00:30) is ENB procedure; the time (00:00:31 to 00:00:51) is the EBUS feature of the lesion; the time (00:00:52 to 00:00:59) is the biopsy process with the guidance of X-ray; the time (00:01:00 to 00:01:07) is brushing process with the guidance of X-ray. ENB, electromagnetic navigation bronchoscopy; EBUS, endobronchial ultrasound; TBLB, transbronchial lung biopsy. Available online: <http://www.asvide.com/articles/1570>

evidences of specimens obtained by ENB procedure and/or other means. If specimens obtained by ENB procedure had definite malignant histological or cytological pathologic evidence, or had characteristic pathology or microbiological evidence of benign disease that was confirmed by the follow-up treatment, they were considered to be diagnosed by ENB. Otherwise, if the specimens gained from ENB did not have specific benign or malignant pathological evidence or specimens were unqualified, they would not be viewed as diagnosed by ENB. For these specimens, the final diagnosis were made by repeated biopsy of ENB or additional procedures, including CT-guided TTNA, surgical biopsy, or clinical and imaging follow-up. All patients received treatment according to the diagnosis made by the methods above and received follow-up for 12 months to review whether the diagnosis was right or not simultaneously.

Cumulative Sum (CUSUM) analysis

The CUSUM method has been widely provided for quantitative evaluation of the learning curve (14-16), which was used in assessing learning curve based on navigation time, total operation time and diagnostic yield in our study. Navigation time was defined as the time from registration completed to the LG reaching the nodule. Total operation time was defined as the time from the bronchoscope passing through the glottis to getting out of the glottis. Diagnostic

yield was the accuracy of the final diagnosis that was proved histopathologically or clinically. The CUSUM is the accumulation of differences between each data and the average of all data. All cases were ordered chronologically to calculate the CUSUM and a power function was approximated. CUSUM was defined as $\sum(X_i - X_0)$, where X_i is individual attempt and X_0 is the reference or target value for the procedure. For the procedure time, X_i and X_0 were the procedure time of each case and the mean procedure time of all cases, respectively. Positive slope means a long procedure time, and negative slope means procedure time decreasing. For the diagnostic yield, X_0 was defined as the overall diagnostic yield, with $X_i = 1$ for diagnostic procedure and $X_i = 0$ for nondiagnostic procedure. Positive slope means diagnostic procedure, and negative slope means nondiagnostic procedure.

Statistical analysis

All statistical analysis was performed using the SPSS version 20.0 (IBM, New York, United States). The results of categorical variables were presented as percentage and continuous variables were presented as mean \pm SD (range). Comparison of the continuous variables and categorical variables was performed using *t*-test or correlation test and Chi-square test or Fisher's exact test, respectively. P value less than 0.05 was considered statistically significant.

Results

Baseline characteristics of the patients and the nodules

Forty patients including 40 nodules were enrolled in the study, of whom 23 (57.5%) were females. The mean age was 59.0 ± 8.7 years, ranging from 39 to 77 years. The mean diameter of the 40 nodules was 21.1 ± 5.3 mm, ranging from 11.0 to 29.7 mm. Characteristics of pulmonary nodules are summarized in *Table 1*.

Diagnostic yield

ENB was successfully performed on the 40 nodules and the final diagnosis was described on *Table 2*. The nearest distance from the sensor probe of the LG to the targeted nodule ranged from 0.1 to 1.6 cm with the average distance of 0.8 ± 0.4 cm. Thirty-three of the 40 nodules (82.5%) were diagnosed by ENB, of which 27 were malignant, 6 were benign. The remaining 7 nodules (17.5%) including 4

Table 1 Characteristics of pulmonary nodules (n=40)

Variables	Data
Size (mm), mean \pm SD (range)	21.1 \pm 5.3 (11.0–29.7)
Lesion location	
Upper lobe	20 (50.0%)
Middle lobe/lingula	6 (15.0%)
Lower lobe	14 (35.0%)
Lesion location from the hilum	
Central	5 (12.5%)
Intermediate	9 (22.5%)
Peripheral	26 (65.0%)
Distance to pleura (mm), mean \pm SD (range)	17.1 \pm 9.9 (0–44.3)

Table 2 Final diagnosis of all nodules (n=40)

Diagnosis	Number	Diagnostic yield
By ENB (n=33)		82.5% (33/40)
Malignant disease (n=27)		
Adenocarcinoma	23	
Squamous carcinoma	3	
SCLC	1	
Benign disease (n=6)		
Inflammation	4	
Tuberculosis	1	
Fungal infection	1	
By others (n=7)		17.5% (7/40)
Malignant disease (n=4)		
Adenocarcinoma [†]	3	
Squamous carcinoma [‡]	1	
Benign disease (n=3)		
Inflammation [§]	2	
Tuberculosis [¶]	1	

[†], Surgery (n=2), TTNA (n=1); [‡], TTNA n (n=1); [§], clinical and imaging follow up (n=2); [¶], clinical and imaging follow up (n=1). ENB, electromagnetic navigation bronchoscopy; SCLC, small cell lung cancer; TTNA, transthoracic needle aspiration.

malignant nodules and 3 benign nodules were nondiagnostic by ENB and finally proved by other diagnostic procedures. The diagnostic yields of ENB in diagnosing malignant and benign nodules were 87.1% (27/31) and 66.7% (6/9), respectively.

The factors, including gender, age, lesion size, lesion location, lesion location from the hilum, relationship between the airway and the nodule and distance from the nodule to the visceral pleura, that may affect the diagnostic yield were analyzed. And it turned out to be no statistical significance between these factors and diagnostic yield finally (*Table 3*).

Learning curve analysis

The navigation time of ENB ranged from 3.1 to 15.2 min with the mean time of 8.1 \pm 3.2 min and the total operation time ranged from 18.6 to 32.6 min with the mean time of 24.6 \pm 4.1 min. The navigation time and total operation time had no correlation with the lesion size analyzed using correlation test ($P=0.71$ and 0.76 , respectively). The raw navigation times of all cases were plotted in chronological order (*Figure 3A*). The CUSUM learning curve based on navigation time was plotted, which was best modeled as a third-order polynomial with a high R^2 value of 0.8856 (*Figure 3B*). The raw total operation times of all cases were plotted in chronological order (*Figure 4A*). The CUSUM learning curve based on total operation time was plotted, which was best modeled as a third-order polynomial with a high R^2 value of 0.9304 (*Figure 4B*). According to the change in the slope of *Figure 3B* and *Figure 4B*, the CUSUM learning curve based on navigation time and total operation time can be divided into two unique phases with the initial 14 cases as phase 1 and the final 26 cases as phase 2. Comparisons of characteristics have no statistical significance between the two consecutive phases (*Table 4*).

The CUSUM learning curve based on diagnostic yield was plotted, which could be modeled as a five-order polynomial with a R^2 value of 0.503 and the shape of the curve did not demonstrate an obvious learning curve (*Figure 5*).

IHC and driver gene analysis

In our study, IHC were performed in 14 samples including

Table 3 Univariate analysis of variables conditioning diagnostic yield

Variables	Diagnostic (n=33)	Nondiagnostic (n=7)	χ^2 (t)	P
Gender			$\chi^2=0.74$	0.43
Male	13	4		
Female	20	3		
Age (years), mean \pm SD (range)	58.8 \pm 8.3 (41.0–77.0)	60.1 \pm 10.8 (39.0–71.0)	t=0.38	0.71
Size (mm), mean \pm SD (range)	20.9 \pm 5.4 (11.0–29.4)	22.1 \pm 5.6 (14.3–29.7)	t=0.55	0.58
Lesion location			$\chi^2=0.24$	0.89
Upper lobe	17	3		
Middle lobe/lingula	5	1		
Lower lobe	11	3		
Lesion location from the hilum			$\chi^2=5.05$	0.08
Central	3	2		
Intermediate	6	3		
Peripheral	24	2		
Relationship [†]			$\chi^2=0.06$	1.00
Leading	25	5		
Adjacent	8	2		
Distance to pleura (mm), mean \pm SD (range)	16.2 \pm 9.3 (0–44.3)	21.2 \pm 12.4 (8.7–44.2)	t=1.21	0.24

[†], Relationship between the airway and the nodule according to the chest CT imaging.

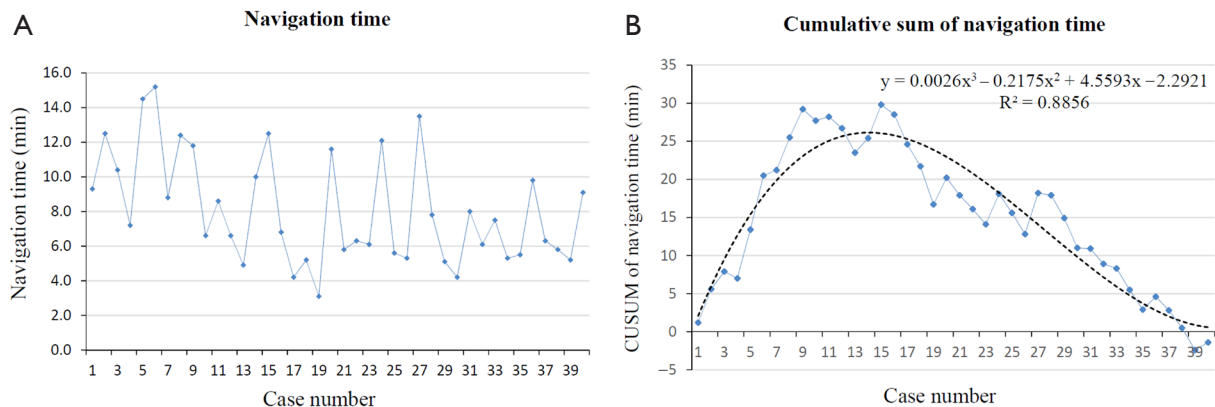


Figure 3 Learning curve based on navigation time. (A) Navigation time plotted against case number; (B) CUSUM of navigation time plotted against case number (solid line with marked point). The dashed line represents the curve of best fit for the plot (a third-order polynomial with equation CUSUM = 0.0026 case number³ - 0.2175 case number² + 4.5593 case number - 2.2921; $R^2 = 0.8856$). CUSUM, cumulative sum.

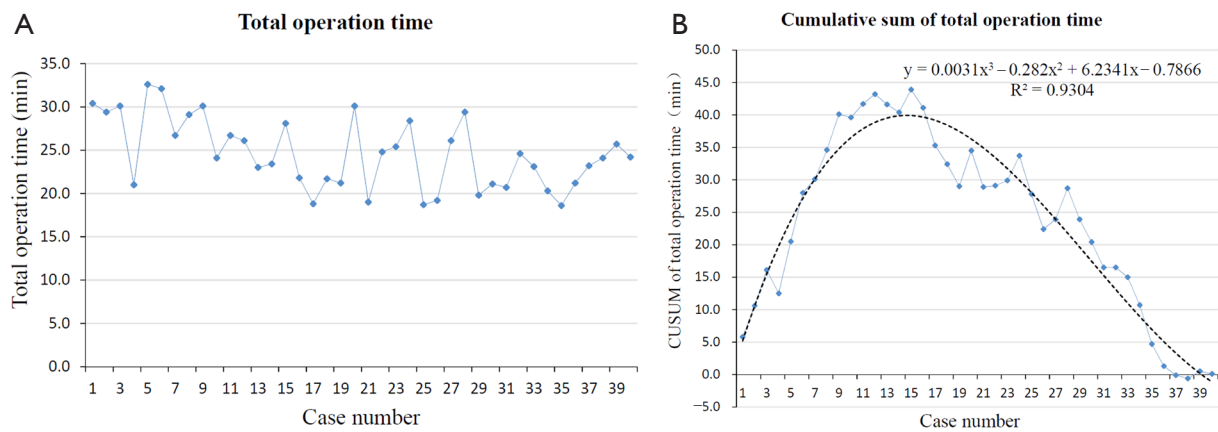


Figure 4 Learning curve based on total operation time. (A) Total operation time plotted against case number; (B) CUSUM of total operation time plotted against case number (solid line with marked point). The dashed line represents the curve of best fit for the plot (a third-order polynomial with equation CUSUM = 0.0031 case number³ - 0.282 case number² + 6.2341 case number - 0.7866; R² = 0.9304). CUSUM, cumulative sum.

Table 4 Comparisons of characteristics between two consecutive phases

Variables	Phase 1	Phase 2	χ^2 (t)	P
Gender			$\chi^2=1.71$	0.32
Male	4	13		
Female	10	13		
Age (years), mean \pm SD (range)	60.7 \pm 8.8 (41.0–77.0)	58.1 \pm 8.6 (39.0–70.0)	t=0.92	0.36
Size (mm), mean \pm SD (range)	19.3 \pm 5.4 (11.0–26.0)	22.1 \pm 5.6 (11.1–29.7)	t=1.62	0.11
Lesion location			$\chi^2=0.82$	0.67
Upper lobe	6	14		
Middle lobe/lingula	3	3		
Lower lobe	5	9		
Lesion location from the hilum			$\chi^2=0.07$	0.97
Central	2	3		
Intermediate	3	6		
Peripheral	9	17		
Relationship [†]			$\chi^2=1.32$	0.28
Leading	9	21		
Adjacent	5	5		
Distance to pleura (mm), mean \pm SD (range)	15.8 \pm 11.5 (0–44.2)	17.8 \pm 9.2 (0–44.3)	t=0.58	0.56

[†], Relationship between the airway and the nodule according to the chest CT imaging.

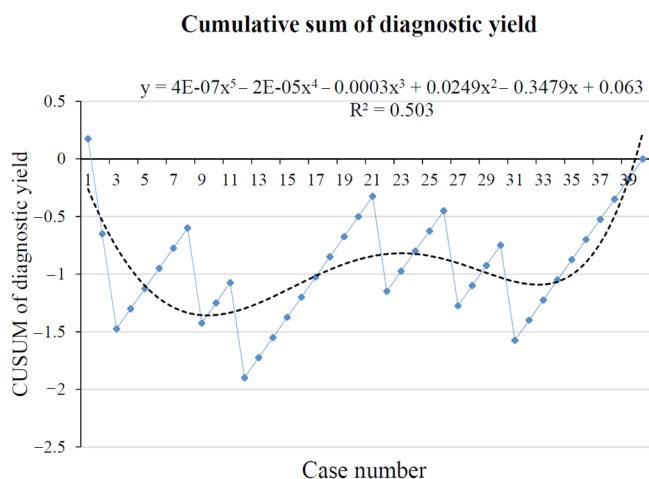


Figure 5 CUSUM of diagnostic yield plotted against case number (solid line with marked point). The dashed line represents the curve fit for the plot (a five-order polynomial with equation $CUSUM = 4E-07 \text{ case number}^5 - 2E-05 \text{ case number}^4 - 0.0003 \text{ case number}^3 + 0.0249 \text{ case number}^2 - 0.3479 \text{ case number} + 0.063$; $R^2 = 0.503$). CUSUM, cumulative sum.

12 adenocarcinomas and 2 squamous cell carcinomas. All of the adenocarcinomas were TTF-1 and CK positive and P40 negative. All of the squamous cell carcinomas were P40 and CK positive and TTF-1 negative.

Driver gene testing using samples gained from ENB was performed in 10 patients diagnosed with lung adenocarcinomas that cannot undergo surgery. EGFR mutations were found in 6 cases including 4 exons 19 and 2 exons 21. No ALK and ROS1 gene fusions were found in these 10 samples. All samples were adequate for IHC and driver gene testing.

Safety

No obvious complications, such as pneumothorax and bleeding, occurred in 40 patients after the procedure in the study.

Discussion

ENB has been proved to be a useful method in diagnosing PPLs (8-10), the pooled sensitivity and specificity was 82% and 100% (17). But operational expertise and learning curve have limited its widespread utilization. Several studies have referred that it took time to train for the use of ENB (12,18-20), but were not designed as learning curve. Lamprecht

et al. (8) reported a steep learning curve with a diagnostic yield of 80% and 87.5% for the first 30 and last 30 procedures, respectively. But these procedures were performed by three bronchoscopists and could not separately reflect learning curve of one bronchoscopist. There were no detailed data available of statistical difference on individual learning curve. Makris *et al.* (21) reported no significant learning curve was observed for each operator separately. The lesion size in the study varied much and the relationship between the lesion and the bronchus was not clear, which lead to some lesions to be diagnosed easily and some difficultly. The study was our preliminary experience in ENB diagnosing peripheral pulmonary nodules and was designed as a learning curve of ENB. The lesion size was limited in a certain range and all the lesions had bronchus leading to or adjacent to on the thin slice chest CT imaging in order to make the difficulty of these procedures equally and increase comparability of the results. GGO was excluded from the study for its difficulty in biopsy and diagnosis.

The training of ENB covers planning, registration, navigation and sampling. As previously described (18), accurate pre-procedure planning of pathways leading to the target lesion was very important to the success of the procedure, and this is highly dependent on the quality of the pre-procedure CT scans. New operators can benefit from hands-on training, standardized lecture, videos of ENB procedure, observing on-the-spot ENB operation, procedural simulation models and *in vivo* animal training before attempting clinical application of ENB. The pulmonologist in our study had took standardized lecture, watched some videos of ENB and observed some on-the-spot ENB operations before the study.

The learning curve was assessed by navigation time, total operation time and diagnostic yield in our study. The navigation time and total operation time in our study was in accordance with previous studies (22,23). We first plotted the raw data by chronological cases and then drew the CUSUM graph, generating a polynomial curve based on the CUSUM graph. Both the CUSUM graphs of navigation time and total operation time were best fitted third-order polynomial curves with the slope changed at 14 cases ($R^2 > 0.8$), and the basic characteristics have no statistical significance between the initial 14 cases and the final 26 cases, which suggested ENB had an obvious learning curve based on navigation time and total operation time. The CUSUM graphs of diagnostic yield was fitted with a five-order polynomial curves ($R^2 = 0.503$). The curve did not demonstrate an obvious learning curve, which can

be explained by the following reasons. First, all procedures in our study were performed by the same physician who had abundant experience in TBLB with the guidance of X-ray and radial endobronchial ultrasound (R-EBUS). What we were unfamiliar with was the system of ENB. The diagnostic yield of ENB in diagnosing pulmonary nodules was related to one's skill of TBLB, which did not change much as long as the EWC reached the nodule. Second, the sample size was small in our study, which led to the diagnostic yield prone to no difference in statistics. Finally, the nodules enrolled were suspected of malignancy, which was easy to diagnose. In short, an experienced pulmonologist can finish the training of ENB after 14 procedures and gained a satisfied diagnosis results.

A meta-analysis of ENB reported the diagnostic yield of ENB in diagnosing PPLs ranged from 55.7% to 87.5%, and the pooled diagnostic yield was 64.9% (24). The meta-analysis also reported that the following several factors could increase the diagnostic yield of ENB in diagnosing PPLs, including nodule location in the upper or middle lobes, greater nodule size, lower registration error, presence of a bronchus sign on CT imaging, combined use of an ultrasonic radial probe, and catheter suctioning as a sampling technique. In our study, all nodules had bronchus leading to or adjacent to, and multiple locating method, including R-EBUS and fluoroscopy, and multiple sampling means, including brushing, biopsy and flushing, were applied in our study. The overall diagnostic yield of our study was 82.5%, higher than the pooled diagnostic yield, which means we had overcome the learning curve. While the diagnostic yield was a little lower than the studies of Lamprecht *et al.* (8) and Pearlstein *et al.* (20), which may be attributed to the reason that ROSE was not applied in our study as it was not done routinely in our hospital. ROSE can increase the diagnostic yield, which was reported by previous studies (25–27).

Personalized therapy plays an important role for tumor patients. Scagliotti *et al.* (28) have reported that patients have different response to the chemotherapy based on their different histologic types. In addition, international association for the study of lung cancer, American thoracic society and European respiratory society (29) have pointed out that molecular markers in predicting response to therapy has become more prominent. It recommends that IHC should be applied to classify NSCLCs in patients with advanced-stage if the tumor cannot be classified based on light microscopy alone. And tissue specimens should be managed for molecular studies to guide therapy for

patients with advanced nonsquamous NSCLCs. If tumor tissue is inadequate for molecular testing, there may be a need to rebiopsy the patient in order to perform testing that will guide therapy (30). IHC and driver gene testing were performed in 14 (35.0%) and 10 (25.0%) patients, respectively, in our study. All samples in our study were adequate for both histologic subtyping and driver gene testing, which was consistent with the studies of Ha *et al.* (31).

The meta-analysis of ENB reported that pneumothorax occurred in 3.1% of the patients with 1.6% required chest tube drainage and minor or moderate bleeding was reported in 0.9% of the patients, none of them requiring specific treatment (24). Similarly, there were no severe complications observed in our study. In a word, ENB has turned out to be a safe technology for diagnosing PPLs.

There are some limitations in the study. First, it was a single center's study and the data in our study were from a pulmonologist with rich experience in TBLB, making it unclear to generalize other less experienced pulmonologist. Although there exist some biases in the study, it still establishes a foundation for studies about the learning curve of ENB for pulmonologists experienced in TBLB. Second, some diseases in the study lacked definitive pathological diagnosis, and the final diagnosis was made by clinical and imaging follow-up. Third, the sample size was small and larger scaled and more generalized studies are needed to evaluate the learning curve further. Last but not the least, the study was not ENB alone. R-EBUS and fluoroscopy were used in the study, because ENB was a navigational tool and was often performed with tools confirming the lesion especially initially used.

Conclusions

ENB has been proven to be a safe technology with a high diagnostic yield and can be preliminary grasped after a short period of training. The learning curve based on procedure time could be stable after 14 procedures and there was no obvious learning curve based on diagnostic yield for a pulmonologist experienced in TBLB. The specimens obtained from ENB are adequate for histologic subtyping and driver gene testing.

Acknowledgments

Funding: This work was supported by Shanghai Chest Hospital key project (2014YZDC20200), Shanghai Municipal Hospitals' Rising and Leading Technology

Program (SHDC12015115), Scientific Research Program by Science and Technology Commission of Shanghai Municipality (15441900502, 15411964300).

Footnote

Conflicts of Interest: All authors have completed the ICMJE uniform disclosure form (available at <http://dx.doi.org/10.21037/tcr.2017.05.39>). The authors have no conflicts of interest to declare.

Ethical Statement: The authors are accountable for all aspects of the work in ensuring that questions related to the accuracy or integrity of any part of the work are appropriately investigated and resolved. The study was conducted in accordance with the Declaration of Helsinki (as revised in 2013). The study was approved by the local ethics committee and the ethics approval number was KS1530. All the patients participating in the study were provided with written informed consent.

Open Access Statement: This is an Open Access article distributed in accordance with the Creative Commons Attribution-NonCommercial-NoDerivs 4.0 International License (CC BY-NC-ND 4.0), which permits the non-commercial replication and distribution of the article with the strict proviso that no changes or edits are made and the original work is properly cited (including links to both the formal publication through the relevant DOI and the license). See: <https://creativecommons.org/licenses/by-nc-nd/4.0/>.

References

1. Torre LA, Bray F, Siegel RL, et al. Global cancer statistics, 2012. *CA Cancer J Clin* 2015;65:87-108.
2. National Lung Screening Trial Research Team, Church TR, Black WC, et al. Results of initial low-dose computed tomographic screening for lung cancer. *N Engl J Med* 2013;368:1980-91.
3. Gould MK, Donington J, Lynch WR, et al. Evaluation of Individuals With Pulmonary Nodules: When Is It Lung Cancer? Diagnosis and Management of Lung Cancer, 3rd ed: American College of Chest Physicians Evidence-Based Clinical Practice Guidelines. *Chest* 2013;143:e93S-120S.
4. Baaklini WA, Reinoso MA, Gorin AB, et al. Diagnostic yield of fiberoptic bronchoscopy in evaluating solitary pulmonary nodules. *Chest* 2000;117:1049-54.
5. Tomiyama N, Yasuhara Y, Nakajima Y, et al. CT-guided needle biopsy of lung lesions: a survey of severe complication based on 9783 biopsies in Japan. *Eur J Radiol* 2006;59:60-4.
6. Gasparini S, Ferretti M, Secchi EB, et al. Integration of transbronchial and percutaneous approach in the diagnosis of peripheral pulmonary nodules or masses. Experience with 1,027 consecutive cases. *Chest* 1995;108:131-7.
7. Rivera MP, Mehta AC, Wahidi MM. Establishing the diagnosis of lung cancer: Diagnosis and management of lung cancer, 3rd ed: American College of Chest Physicians evidence-based clinical practice guidelines. *Chest* 2013;143:e142S-65S.
8. Lamprecht B, Porsch P, Wegleitner B, et al. Electromagnetic navigation bronchoscopy (ENB): Increasing diagnostic yield. *Respir Med* 2012;106:710-5.
9. Mahajan AK, Patel S, Hogarth DK, et al. Electromagnetic navigational bronchoscopy: an effective and safe approach to diagnose peripheral lung lesions unreachable by conventional bronchoscopy in high-risk patients. *J Bronchology Interv Pulmonol* 2011;18:133-7.
10. Eberhardt R, Anantham D, Ernst A, et al. Multimodality bronchoscopic diagnosis of peripheral lung lesions: A randomized controlled trial. *Am J Respir Crit Care Med* 2007;176:36-41.
11. Schwarz Y, Greif J, Becker HD, et al. Real-time electromagnetic navigation bronchoscopy to peripheral lung lesions using overlaid CT images: the first human study. *Chest* 2006;129:988-94.
12. Becker HD, Herth F, Ernst A, et al. Bronchoscopic biopsy of peripheral lung lesions under electromagnetic guidance: a pilot study. *J Bronchology Interv Pulmonol* 2005;12:9-13.
13. Jiayuan Sun, Fangfang Xie, Xiaoxuan Zheng, et al. Video of ENB-EBUS-X-ray-TBLB procedure. *Asvide* 2017;4:261. Available online: <http://www.asvide.com/articles/1570>
14. Jeon HH, Lee HS, Youn YH, et al. Learning curve analysis of colorectal endoscopic submucosal dissection (ESD) for laterally spreading tumors by endoscopists experienced in gastric ESD. *Surg Endosc* 2016;30:2422-30.
15. Oh D, Park DH, Song TJ, et al. Optimal biliary access point and learning curve for endoscopic ultrasound-guided hepaticogastrostomy with transmural stenting. *Therap Adv Gastroenterol* 2017;10:42-53.
16. Zhou J, Shi Y, Qian F, et al. Cumulative summation analysis of learning curve for robot-assisted gastrectomy in gastric cancer. *J Surg Oncol* 2015;111:760-7.
17. Zhang W, Chen S, Dong X, et al. Meta-analysis of the diagnostic yield and safety of electromagnetic

- navigation bronchoscopy for lung nodules. *J Thorac Dis* 2015;7:799-809.
18. Leong S, Ju H, Marshall H, et al. Electromagnetic navigation bronchoscopy: A descriptive analysis. *J Thorac Dis* 2012;4:173-85.
 19. Gildea TR, Mazzone PJ, Karnak D, et al. Electromagnetic navigation diagnostic bronchoscopy: a prospective study. *Am J Respir Crit Care Med* 2006;174:982-9.
 20. Pearlstein DP, Quinn CC, Burtis CC, et al. Electromagnetic navigation bronchoscopy performed by thoracic surgeons: one center's early success. *Ann Thorac Surg* 2012;93:944-9.
 21. Makris D, Scherpereel A, Leroy S, et al. Electromagnetic navigation diagnostic bronchoscopy for small peripheral lung lesions. *Eur Respir J* 2007;29:1187-92.
 22. Eberhardt R, Anantham D, Herth F, et al. Electromagnetic navigation diagnostic bronchoscopy in peripheral lung lesions. *Chest* 2007;131:1800-5.
 23. Eberhardt R, Morgan RK, Ernst A, et al. Comparison of suction catheter versus forceps biopsy for sampling of solitary pulmonary nodules guided by electromagnetic navigational bronchoscopy. *Respiration* 2010;79:54-60.
 24. Gex G, Pralong JA, Combescure C, et al. Diagnostic yield and safety of electromagnetic navigation bronchoscopy for lung nodules: a systematic review and meta-analysis. *Respiration* 2014;87:165-76.
 25. Lamprecht B, Porsch P, Pirich C, et al. Electromagnetic navigation bronchoscopy in combination with PET-CT and rapid on-site cytopathologic examination for diagnosis of peripheral lung lesions. *Lung* 2009;187:55-9.
 26. Karnak D, Ciledağ A, Ceyhan K, et al. Rapid on-site evaluation and low registration error enhance the success of electromagnetic navigation bronchoscopy. *Ann Thorac Med* 2013;8:28-32.
 27. Wilson DS, Bartlett RJ. Improved diagnostic yield of bronchoscopy in a community practice: combination of electromagnetic navigation system and rapid on-site evaluation. *Journal of Bronchology* 2007;14:227-32.
 28. Scagliotti GV, Parikh P, von Pawel J, et al. Phase III study comparing cisplatin plus gemcitabine with cisplatin plus pemetrexed in chemotherapy-naïve patients with advanced-stage non-small-cell lung cancer. *J Clin Oncol* 2008;26:3543-51.
 29. Travis WD, Brambilla E, Noguchi M, et al. International association for the study of lung cancer/american thoracic society/european respiratory society international multidisciplinary classification of lung adenocarcinoma. *J Thorac Oncol* 2011;6:244-85.
 30. Travis WD, Brambilla E, Noguchi M, et al. Diagnosis of lung cancer in small biopsies and cytology: implications of the 2011 International Association for the Study of Lung Cancer/American Thoracic Society/European Respiratory Society classification. *Arch Pathol Lab Med* 2013;137:668-84.
 31. Ha D, Choi H, Almeida FA, et al. Histologic and molecular characterization of lung cancer with tissue obtained by electromagnetic navigation bronchoscopy. *J Bronchology Interv Pulmonol* 2013;20:10-5.

Cite this article as: Sun J, Xie F, Zheng X, Jiang Y, Zhu L, Mao X, Han B. Learning curve of electromagnetic navigation bronchoscopy for diagnosing peripheral pulmonary nodules in a single institution. *Transl Cancer Res* 2017;6(3):541-551. doi: 10.21037/tcr.2017.05.39